STUDIES ON CHROMOPHORE COUPLING IN ISOLATED PHYCOBILIPROTEINS

II. Picosecond Energy Transfer Kinetics and Time-resolved Fluorescence Spectra of C-Phycocyanin from *Synechococcus 6301* as a Function of the Aggregation State

ALFRED R. HOLZWARTH, JOACHIM WENDLER, AND GEORG W. SUTER
Max-Planck-Institut für Strahlenchemie, Stiftstr. 34–36, D-4330 Mülheim a.d. Ruhr, West Germany

ABSTRACT The fluorescence kinetics of C-Phycocyanin in the monomeric, trimeric, and hexameric aggregation states has been measured as a function of the emission wavelength with picosecond resolution using the single-photon timing technique. All the decay curves measured at the various emission wavelengths were analyzed simultaneously by a global data analysis procedure. A sum of four exponentials was required to fit the data for the monomers and trimers. Only in the case of the hexamers, a three-exponential model function proved to be nearly sufficient to describe the experimental decays. The lifetime of those fluorescence components reflecting energy transfer decreased with increasing aggregation. This is due to the increased number of efficient acceptor molecules next to a donor in the higher aggregates. In all aggregates the shortest-lived component, ranging from 50 ps for monomer to 10 ps for hexamers, is observed as a decay term (positive amplitude) at short emission wavelength. At long emission wavelength it turns into a rise term (negative amplitude). The lifetime of a second ps-component ranges from 200 ps for monomers to 50 ps for hexamers. The long-lived (ns) fluorescence is inhomogeneous in monomers and trimers, showing two lifetimes of ~0.6 and 1.3 ns. The latter one carries the larger amplitude. The amplitudes of the kinetic components in the fluorescence decays are presented as time-resolved component spectra. A theoretical model has been derived to rationalize the observed fluorescence kinetics. Using symmetry arguments, it is shown that the fluorescence kinetics of C-Phycocyanin is expected to be characterized by three exponential kinetic components, independent of the aggregation state. An analytical expression is derived, which allows us to gain a detailed understanding of the origin of the different kinetic components and their associated time-resolved spectra. Numerical calculations of time-resolved spectra are compared with the experimental data.

INTRODUCTION

C-Phycocyanin (C-PC) is one of the phycobiliproteins that form the light-harvesting antenna in cyanobacteria and red algae, the so-called phycobilisomes (PBS) (1–6). In vitro it occurs in monomeric, trimeric, or hexameric aggregation states (7–10). In PBS of *Synechococcus 6301* (S 6301), C-PC forms long rods that consist of 3–4 hexameric units (11, 12). The aggregation to states higher than trimeric seems to depend on the presence of uncolored linker peptides (12, 13). Phycobiliproteins generally contain chromophores with different absorption and fluorescence spectra. The short-wavelength absorbing chromophores are often called "sensitizing" (S)-chromophores, because they are believed to transfer their excitation energy to the long-wavelength absorbing chromophores, which are thus termed "fluorescing" (F)-chromophores (14). The concept of S-chromophores and F-chromophores is only a relative one, since F-chromophores may turn into S-chromophores upon going to higher aggregation. Monomeric C-PC contains three phycocyanobilin chromophores distributed over two protein subunits. Two of them are contained in the β-subunit and one is contained in the α-subunit (4).

The energy transfer in phycobiliproteins has been studied using steady state fluorescence and fluorescence polarization (14–17) as well as fluorescence lifetime (for recent reviews see references 18 and 19) and kinetic absorption spectroscopy (20–24). Some of these studies revealed the presence of short decay components which were attributed to s→f energy transfer (1, 20, 24–27) or, at high excitation intensities, to exciton annihilation (21, 22, 28). Internal s→f energy transfer in trimeric/hexameric phycobiliproteins has also been held responsible for the fast anisotropy decay in fluorescence (10, 25, 29) and absorption (23, 24). From the concept of short-wavelength absorbing S-chromophores and longer-wavelength absorbing F-chromophores, risetimes (negative amplitude components) are predicted in the fluorescence kinetics upon preferential

Address all correspondence to Dr. Holzwarth.

excitation of the S-chromophores and preferential detection of the fluorescence from the F-chromophores. Such risetimes have been observed so far only in B-phycoerythrin (27), in C-Phycocyanin from *Mastigocladus* (30), and in phycocyanin 612 from *Cryptophyceae* (31).

For the particular case of isolated C-PC, researchers found a complex dependence of the fluorescence decay and polarization parameters on the aggregation state and the temperature (10, 16, 20, 29). The inhomogeneity in the long-lived (ns) fluorescence decay components of C-PC monomers (16) and α-subunits (16, 29) has been attributed to an inhomogeneity in the conformational state of the protein and/or chromophores in these samples. Our own studies of intact PBS from *Synechococcus 6301* and the mutant *AN 112* showed fast decay components with lifetimes in the range of 10 to 20 ps, which were attributed preferentially to s→f energy transfer within C-PC trimeric and hexameric units (23, 24, 26). In a study of trimeric C-PC from *Mastigocladus laminosus* we found, among other decay components, fast fluorescence decay and rise terms with lifetimes in the range of 22 to 36 ps (30).

In this study we further clarify the excited state properties and energy transfer kinetics of C-PC from *Synechococcus 6301* and their dependence on the aggregation state. Recording time-resolved fluorescence spectra with picosecond resolution and to evaluate these data by a global data analysis procedure (30, 32, 33) should be suitable to gain more insight into the complex decay phenomena and the chromophore coupling in this phycobiliprotein. This technique should also resolve complications met in previous studies, which were more limited in either their time-resolution and/or their capability for multicomponent resolution.

MATERIALS AND METHODS

Isolation of C-Phycocyanin

Hexameric C-PC was isolated after partial dissociation of PBS by the following procedure. PBS from *Synechococcus 6301* (S 6301) were isolated as described previously (26). The PBS were diluted into 0.325 M phosphate buffer pH = 5.5. The mixture was layered on continuous sucrose gradients 0.2–0.9 M in the same buffer and ultracentrifugation was carried out (26,000 rpm; SW 28 rotor, Beckman Instruments, Inc., Fullerton, CA). Three bands separated after 21 h of centrifugation. The upper band contained mixtures of low molecular weight C-PC and allophycocyanin (APC). The middle band contained pure C-PC, while the lowest band contained higher aggregates of C-PC and APC, probably together with partially dissociated PBS. The analytical ultracentrifugation of the pure C-PC fraction gave a sedimentation coefficient of $S_{20,w}$ = 11, which is consistent with a hexameric aggregation state (7, 10, 29, 34, 35). SDS gel electrophoresis using the system of Laemmli (36) showed that the preparation was free from other biliproteins. Overloaded gels showed that the C-PC was associated with linker peptides of 33,000 and 30,000 molecular weight (mol wt) (13, 37). The linker peptide with a molecular weight of 33,000 was ~4–5 times more abundant than the 30,000-mol-wt.

For the isolation of trimeric C-PC, the cells of S 6301 were washed in 0.05 M NaK-phosphate buffer, pH 7.0, and then broken in a French press. After centrifugation of the homogenate (JA 21 rotor, 21,000 rpm; Beckman Instruments, Inc.) the blue supernatant was layered onto a continuous sucrose density gradient (0.2–0.9 M) in the same buffer and was run in the ultracentrifuge (SW 28 rotor, 26,000 rpm) at 4°C for 17 h. Five separate bands developed. The middle band contained most of the C-Phycocyanin. The contents of this band were dialyzed against 50 mM phosphate buffer, pH 7.0. The sample was then chromatographed on a hydroxylapatite column (hydroxylapatite spherical, 0.075–0.18 mm). The sample was eluted in the same buffer using a NaCl gradient up to 0.4 M. The C-PC fraction was dialyzed against 50 mM phosphate buffer, pH 7.0, and concentrated. The analytical ultracentrifugation gave a value of $S_{20,w}$ = 5.4, consistent with a trimeric aggregation state (7, 10, 29, 34, 35). SDS gel electrophoresis showed that the trimers were free from linker peptides.

To obtain monomeric C-PC, the trimeric aggregates were dissociated by adding 0.5 M KSCN, a chaotropic agent, in phosphate buffer 50 mM, pH 7.0. By analogy with other reports (10, 29) and from the change in the absorption spectrum (see below), it was expected that the aggregation state in KSCN solution was monomeric. The sedimentation coefficient of $S_{20,w}$ = 2.3 (34, 35) is consistent with that expectation.

Spectroscopic Methods

Absorption spectra were measured on a spectrophotometer (model PE 320; Perkin-Elmer Corp., Norwalk, CT). Corrected fluorescence and fluorescence excitation spectra were recorded on a computer-controlled luminescence spectrometer (Fluorolog; Spex Industries, Inc., Edison, NJ) as described previously (38).

Picosecond fluorescence decays and time-resolved fluorescence spectra were measured by the single-photon-timing technique. The source of picosecond excitation pulses was a synchronously pumped and cavity-dumped dye laser system (Spectra-Physics, Inc., Mountain View, CA). The detection system consisted of a monochromator (DH 10; Jobin Yvon Inc., Longjumeau, France) and a channel-plate photomultiplier (model R1564U-01; Hamamatsu Corp., Middlesex, NJ). The detection bandwidth was 4 nm. The excitation function of our single-photon-timing system was only 40–60 ps wide (full width at half maximum), depending on the tuning conditions. This narrow time response function of our apparatus allows the accurate determination of fluorescence decays down to 5 ps by deconvolution procedures. The wavelength dependent sensitivity factors of the detection system have been determined using a calibrated quartz-halogen lamp (Osram Inc., Essen, West Germany) operated by a constant current power supply. The amplitudes of all time-resolved spectra were corrected using these sensitivity factors. All fluorescence decay measurements were carried out at ambient temperature (22–25°C) under magic angle polarization (isotropic fluorescence) to eliminate interference with time-dependent anisotropy effects. The samples were slowly flowed through the measuring cuvette during the recording of time-resolved data to exclude any possibility for light-induced changes of the sample. All measurements were carried out within 2 d after the isolation of the C-PC. All buffers for the isolation and handling of C-PC contained mercaptoethanol (1 mM) and Na-azide (0.02% wt/vol).

Global Data Analysis

The fluorescence decays were analyzed by a deconvolution procedure based on a global optimization algorithm (32, 33). In this procedure, several fluorescence decays, recorded as a function of a third and independent parameter (in our case the emission wavelength), are deconvoluted and analyzed simultaneously in a single run. This procedure ensures global optimization of the kinetic model to the entire three-dimensional (intensity, time, wavelength) data surface. The global data analysis procedure is expected to greatly enhance the capability for multicomponent resolution and to reduce the statistical errors in lifetimes and amplitudes. This improvement is important in view of the complexity of the fluorescence decays from phycobiliproteins and PBS (30).

The algorithm is based on the assumption that the decay constant (lifetime) τ_i of a particular decay component should be independent of wavelength, while the preexponential factors A_i vary. The fluorescence

decay is described by a sum of exponential functions

$$F(t,\lambda) = \sum_{i=1}^{n} A_i(\lambda) \exp(-t/\tau_i). \quad (1)$$

If the lifetimes are independent of emission wavelength, the dimensionality of the fitting problem can be reduced from $2 \times N \times n$, to $N \times n + n$ by applying the global analysis. Here, N denotes the number of independent measurements at different wavelengths and n is the number of decay components. This reduction in the dimensionality of the free parameter space leads to a substantial improvement in the accuracy of the extracted parameters as well as in the capability for multicomponent resolution. The quality of the fits was judged by a global χ^2-value, individual χ^2-values, and plots of the weighted residuals. The iteration procedure applied in our program is a semilinear Marquardt algorithm (39). The feasibility and reliability of the four-exponential analysis has been tested on a number of simulated data sets with three and four decay components, which mimicked the experimental time-resolved spectra. Poissonian noise had been added to these simulated decay data. These tests confirmed the expected improvement by the global data analysis as compared with the conventional single-decay analysis. In all these simulations the theoretical parameters (amplitudes and lifetimes) were recovered very closely, which makes us confident that the present analysis is reliable.

The amplitudes A_i (Eq. 1) of the kinetic components obtained from the global data analysis procedure were plotted as time-resolved spectra of these individual components. When the spectra of different chromophores

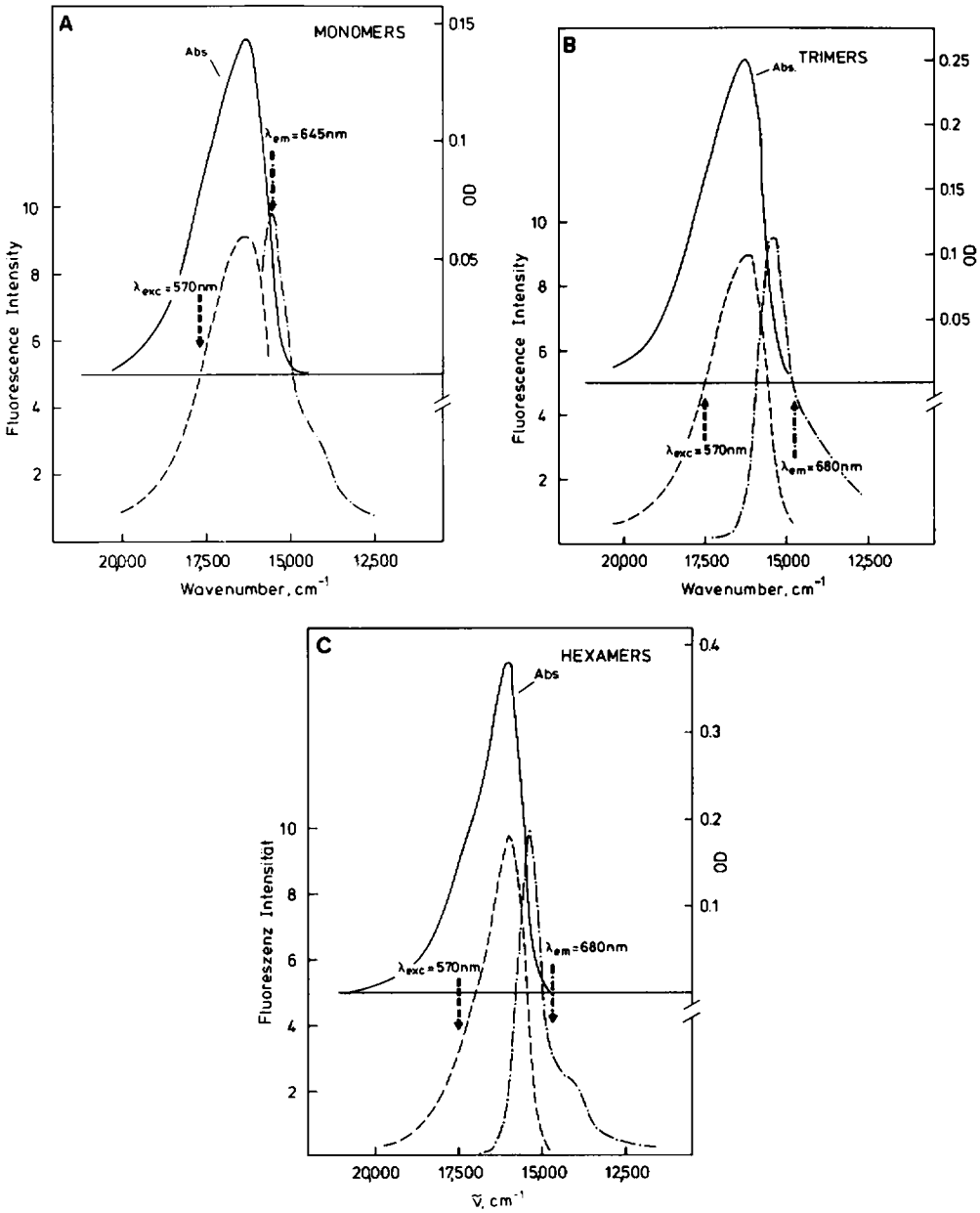

FIGURE 1 Absorption (*full line*), corrected steady state fluorescence excitation (*dashed line*), and fluorescence emission (*dashed-dotted line*) spectra of the three C-PC aggregates: (*A*) monomers, (*B*) trimers, and (*C*) hexamers. The experimental conditions are given in Materials and Methods.

TABLE I
MAXIMA OF THE ABSORPTION, CORRECTED STEADY STATE FLUORESCENCE EMISSION, AND FLUORESCENCE EXCITATION SPECTRA OF THE THREE C-PC AGGREGATES*

Aggregate	$S_{20,w}$	pH	Buffer	$\lambda^{abs}_{max,nm}$	$\lambda^{exc}_{max,nm}$	$\lambda^{em}_{max,nm}$
Monomer	2.3	7.0	50 mM Phosphate	612	612	642
Trimer	5.4	7.0	50 mM Phosphate	615	618	647
Hexamer	11	5.5	0.325 M Phosphate	624	625	651

*The sedimentation coefficients $S_{20,w}$ are also given. Fluorescence measurements have been carried out at ambient temperature (22–25°C).

overlap strongly and there are rise terms present due to energy transfer, as is the case here, it is not generally possible to extract the precise spectral shape of the donor component. Rather, donor-acceptor difference spectra will be observed in this case (See Kinetic Analysis below for further details).

RESULTS

The absorption, steady state fluorescence, and fluorescence excitation spectra of the different aggregates are given in Fig. 1. Maxima of the absorption and fluorescence spectra are compiled in Table I. It can be seen that the absorption and emission maxima shift to longer wavelengths with increase in the aggregation state. Along with the bathochromic shift goes a narrowing of the spectra. This is most pronounced for the hexameric aggregation. All of these observations are consistent with literature data for these different aggregation states (8, 10, 11, 17, 29).

Time-resolved Spectra

Picosecond time-resolved spectra were measured with excitation at λ_{exc} = 590 nm. This wavelength was chosen because preliminary experiments, as well as the data on the absorption and fluorescence of C-PC subunits from (16), indicated that this is the region of maximum absorption of the short-wavelength S-chromophore(s). This is also supported by the very recent deconvolution of the absorption spectra of C-PC from *Mastigocladus* (17). Fluorescence decays were recorded as a function of the emission wavelength at 10 nm intervals. Typical residuals plots and χ^2-values from the global data analysis procedure are shown in Fig. 2, *left* and *right*, for three-exponential and four-exponential model functions in the case of the trimers. These data show that four exponentials are required to describe the fluorescence decays. The three-exponential fit shows large systematic deviations in the residuals. The analysis of the decays from the monomers resulted in very similar residual plots (not shown). The time-resolved spectra for the three aggregates are shown in Figs. 3, *A–C*. The

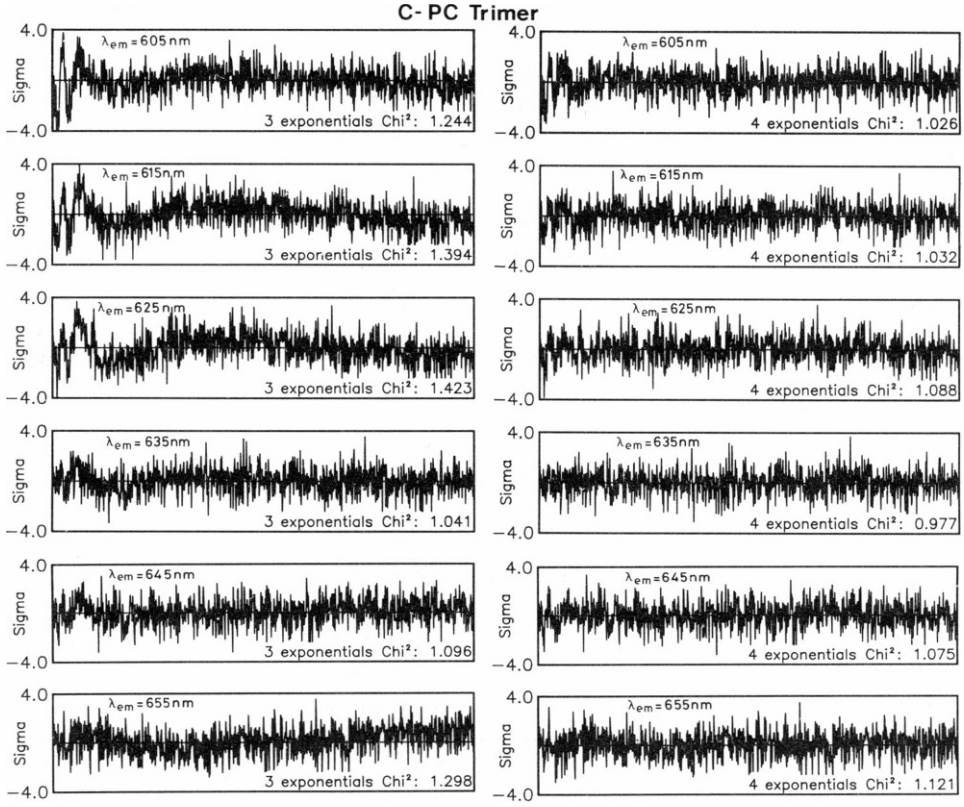

FIGURE 2 Weighted residual plots from the global data analysis of the fluorescence decays from trimers of C-PC for a three-exponential (*left*) and a four-exponential (*right*) model function. The χ^2-values and emission wavelengths are given for each decay. Note the strong systematic deviations from a random distribution in the case of the three-exponential model function.

TABLE II
FLUORESCENCE LIFETIMES (τ, ps) OF THE KINETIC COMPONENTS OF THE AGGREGATES OF C-PC FROM SYNECHOCOCCUS 6301*

Aggregate	τ_1‡	τ_2‡	τ_3‡	τ_4‡	Comments
Monomer	47–53	200	675	1,320–1,350	—
Trimer	35	117–125	600	1,310–1,350	—
Hexamer	10	50	550–570	1,810–1,830	τ_3 has very small amplitude; the kinetics can be described approximately by a three-exponential model also.

*The lifetimes have been calculated using the simultaneous data analysis procedure from six to seven fluorescence decays in each case. The ranges for the lifetimes are those from several independent measurements. Experimental conditions (concentration, temperature, pH, buffer, etc.) were the same as for recording the stationary spectra (Fig. 1); see also Materials and Methods.
‡Maximum errors in the short lifetimes are 10% or ±3 ps, whichever is larger. For the long lifetimes the maximum errors are 5%.

lifetimes of the components obtained from this analysis are collected in Table II.

Monomeric C-Phycocyanin. The shortest lifetime component is 47 ps for the monomer. The associated spectrum has a large positive amplitude (decay term) in the range of 610–620 nm. Above 635 nm, this component turns into a rise term (negative amplitude). This means that the long-wavelength emission has a delayed rise with a time constant of 47 ps. The other three kinetic components have positive amplitudes over the whole wavelength range examined. The largest amplitude is carried by a component with a maximum around 640 nm and a lifetime of ~1.3 ns. Another component (675 ps) has about the same spectrum as the longest-lived component but carries an amplitude that is ~50% smaller. A 200-ps component peaks around 635 nm and differs in spectral shape from the other components.

Trimeric C-Phycocyanin. The component-resolved spectra of the trimers are shown in Fig. 3 *B*. At short emission wavelength a very fast decay (35 ps) with maximum amplitude around 615 nm is observed, which turns into a rise term (negative amplitude) at wavelengths above 630 nm. In addition, we find another short-lived component (120 ps). Its spectrum peaks around 635 nm. The amplitude is positive over almost the entire wavelength range examined, except at the very long-wavelength end (655 nm), where there is a slight indication of a small negative amplitude. Two long-lived decays with lifetimes of 1.3 and 0.6 ns are observed as well with maxima around 645 nm. They have very similar shapes and their amplitude ratio is ~2:1 as in the case of the monomers.

Hexameric C-Phycocyanin. Time-resolved fluorescence spectra of hexameric aggregates were measured as described above (cf. Fig. 3 *C*). The general picture is very similar to the case of trimeric aggregates. The residual plots from the global data analysis procedure still indicate the requirement for a four-exponential model function for a perfect fit. However, in this case, the improvement is only minor as compared with a three-exponential analysis. The intermediate decay (550 ps) is now drastically reduced in amplitude as compared with the trimers and monomers (note the 10-fold expansion factor for the corresponding amplitudes in Fig. 3 *C*), which makes the long-lived fluorescence more homogeneous in the hexamers than in monomers and trimers. This explains the small difference in the quality of the residuals of the three-exponential as compared with the four-exponential analysis for hexamers. Both the long and the short lifetimes are significantly different from the corresponding values of the trimers and monomers. While the short-lived decay components are even shorter (10 and 50 ps), we find the long-lived decay time (1.8 ns) to be considerably increased in comparison to the trimers. The shortest-lived decay component (10 ps) again turns into a risetime (negative amplitude) above 630-nm emission wavelength (cf. Fig. 3 *C*). At the long wavelength edge, also, the 50 ps component goes negative. This effect is now more pronounced than in the case of the trimer.

DISCUSSION

The energy transfer processes between the various chromophores in the three different C-PC aggregates will now be discussed on the basis of the known spectral differences of the various chromophores. A model will be developed that also allows a description of the fluorescence decay both in terms of closed analytical formulae and in the form of more tractable numerical caiculations.

The β-chain of C-PC carries two chromophores with significantly different absorption and emission spectra (7, 17). The sensitizing chromophore with the absorption maximum at ~590–600 nm will be designated as S-chromophore. The spectrum of the other, long-wavelength absorbing, β-chromophore is only slightly red-shifted relative to the one in the α-chain (17). We designate the chromophore with the intermediate spectrum (α-chromophore) as M and the long-wavelength chromophore as F, without, at this stage, making a definite assignment of a specific chromophore in the β-chain and the S and F species. Probably the best spectra for the individual chromophores of C-PC have been deconvoluted by Mimuro et al. (17). We therefore take these spectra as the model

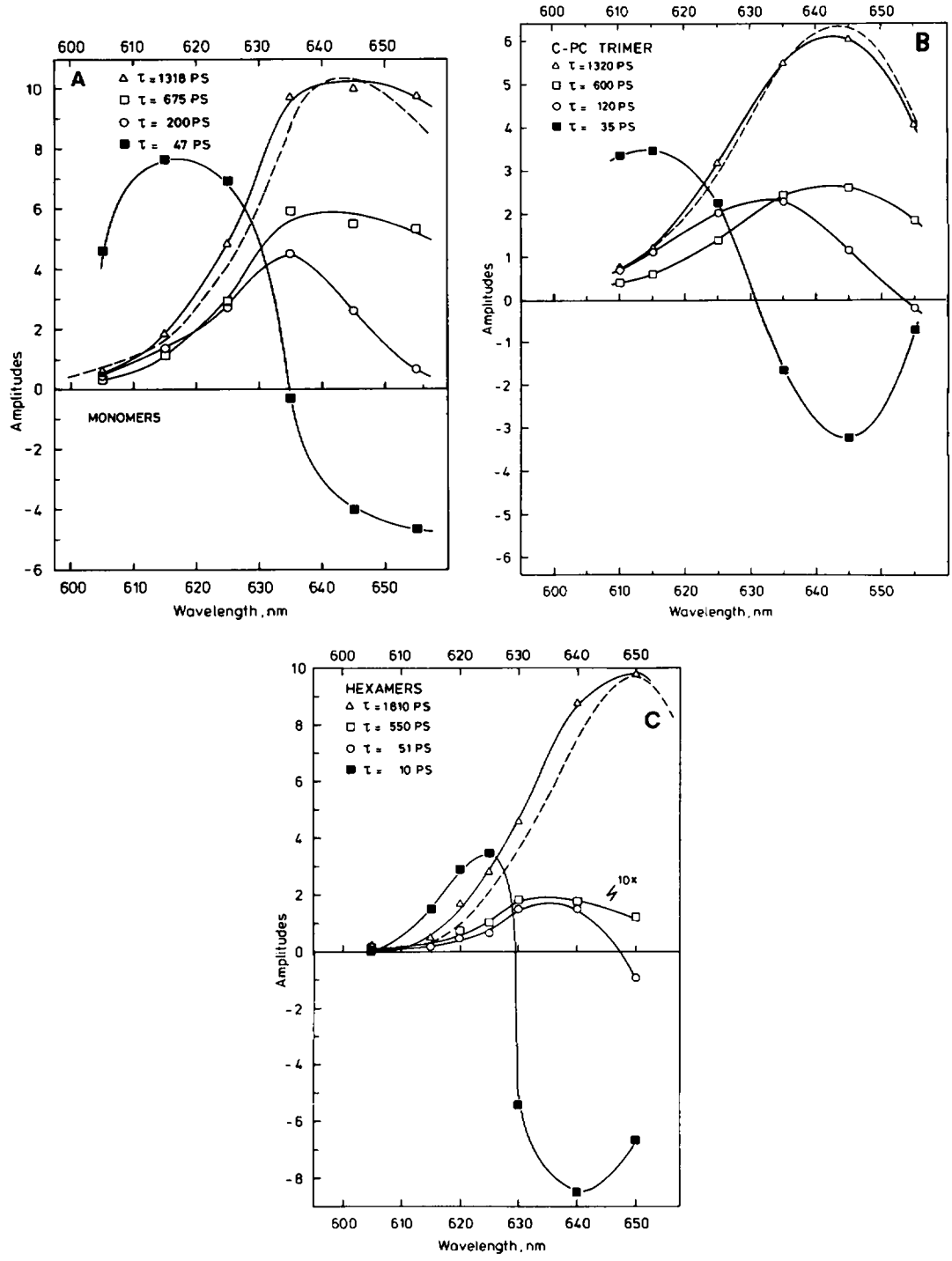

FIGURE 3 Corrected time-resolved component spectra of the fluorescence decays from C-PC aggregates: (*A*) monomers, (*B*) trimers, and (*C*) hexamers. The excitation wavelength was λ_{exc} = 590 mn. The symbols give the data points and the full lines represent the suggested spectra. The dashed lines give the stationary fluorescence spectrum of the corresponding aggregates for comparison (same data as in Fig. 1, *A–C*).

spectra in our calculations. They are collected in Fig. 4. The emission spectrum of the S-chromophore, which has not been separated in Reference 17, has been estimated by taking the same spectral shape and Stokes-shift relative to its absorption maximum as has been measured for the chromophore of the α-chain.

Kinetic Analysis

From the x-ray analysis of C-PC it is known that both trimers and hexamers have a threefold fold symmetry axis. In addition, the hexamers, built up of two trimers in a head-to-head configuration, have three twofold axes perpendicular to the main symmetry axis (40, 41). Thus, trimers and hexamers both contain three groups of (three and six, respectively) symmetrically equivalent chromophores. As shown in another paper (Holzwarth, A. R., and G. W. Suter, manuscript submitted for publication) (see also Appendix), each of these groups can be treated kinetically like a single ("super"-)chromophore or pseudospecies, if one is interested in the isotropic fluorescence

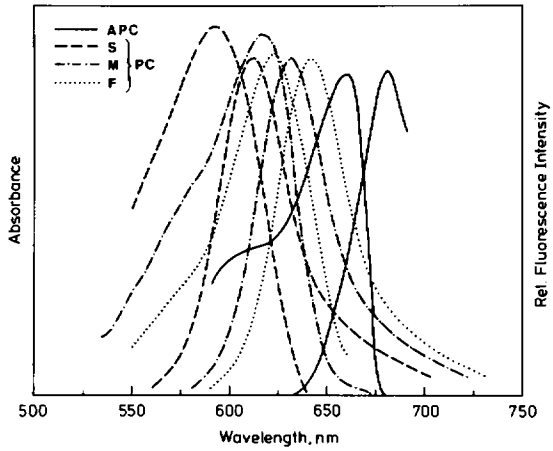

FIGURE 4 The model spectra of C-PC (S, *dashed line;* M, *dashed-dotted line;* F, *dotted line*) used in the model calculations shown in Figs. 5, *A* and *B*. The spectra have been taken from reference 17 (see text).

decay. Under such isotropic detection conditions, one can not differentiate between the contributions from the symmetrically equivalent chromophores. Making use of the irreducible representations of the appropriate symmetry group (C_3 in the case of the trimers and D_3 in the case of the hexamers), a transformation matrix can be constructed by which the kinetic matrices describing the energy transfer among all the chromophores can be transformed using the formalism given in the Appendix (also see Holzwarth, A. R., and G. W. Suter, manuscript submitted for publication, for a more extensive discussion). After transformation of the kinetic matrix, a block diagonal form results which can be reduced to the dimension 3 × 3, i.e., the same dimension as in the case of the monomer. The transformation results in symmetry adapted pseudo-species (linear combinations of the real species) and in a symmetry adapted kinetic matrix. Thus, the corresponding kinetic equations for the trimers and hexamers are formally identical to those describing the transfer in the monomers. The 3 × 3 matrix that results for each aggregate describes a system of coupled linear differential equation with exactly three rate constants, which are obtained by solving for the eigenvalues of the matrix. The corresponding eigenvectors give the amplitudes of the time-resolved spectra. Thus, the isotropic fluorescence kinetics in C-PC will be described by a sum of three exponential components for any one of the different aggregation states. Only the rate constants (lifetimes) and the corresponding time-resolved spectra will depend on the aggregation state.

Analytical Expressions

In addition to the kinetic analysis described above and in the Appendix, which provides the basis for exact numerical calculations of time-resolved spectra, we have also derived the analytical solution of the kinetic equations. Two simplifying approximations have been made for this derivation, however: (*a*) the energy-transfer processes between the chromophores are assumed to be fast as compared with the radiative and radiationless deactivation, and (*b*) the back transfer to the S-chromophore(s) has been neglected. The first assumption is easily justified, while the second one is perhaps not fully realized, i.e., in reality back transfer to the F-chromophore will contribute to some extent. Nevertheless, we use this simplification here because it results in analytical formulae that are still tractable and informative in the sense that they provide the basis for a more qualitative understanding of the kinetics and time-resolved spectra. The general analytical solution, taking into account all rate constants, is very complex and therefore not particularly suitable for a semiquantitative discussion. It is important to realize, however, that these simplifying assumptions do not change the predicted number of kinetic components. Taking into account this back transfer would simply modify to some extent the calculated rate constants. Using numerical calculation on the basis of the matrix formalism described above instead of the analytical derivations, the inclusion of the rate constants describing back transfer is straightforward (Holzwarth, A. R., and G. W. Suter, manuscript submitted for publication). Within these approximations the fluorescence decay observed at λ_{em} upon excitation at λ_{ex} is given by the following formulae, which have been obtained by analytically solving the symmetry adapted matrix equations given in the Appendix:

$$d(\lambda_{em}, t) \propto a_1(\lambda_{em}) \exp -(k_r + k_{nr})t + a_2(\lambda_{em}) \exp - (k_{SM} + k_{SF})t + a_3(\lambda_{em}) \exp - (k_{MF} + k_{FM})t. \quad (2)$$

In the formulae above and in the following, k_r and k_{nr} denote the rate constants for radiative and nonradiative deactivation, which are assumed to be approximately the same for all types of chromophores e^S, e^M, e^F (λ_{em}) are the normalized emission spectra, and ϵ^S, ϵ^M, ϵ^F (λ_{exc}) are the extinction coefficient of the different types of chromophores. Note that in the case of the trimers and hexamers, the rate constants in the second and third terms represent a sum of individual rate constants. For example, $k_2 = k_{SM} + k_{SF}$ is the sum of all the rate constants leading from one individual S-chromophore to all M- and F-chromophores in that aggregate. Likewise, $k_3 = k_{MF} + k_{FM}$ is the sum of all rate constants for transfer between F and M chromophores.

The amplitude terms are given by

$$a_1(\lambda_{em}) = [\epsilon^S + \epsilon^M + \epsilon^F] \cdot \left\{ \left[\frac{1}{2} [k_r^M e^M(\lambda_{em}) + k_r^F e^F(\lambda_{em})] + \frac{(k_{FM} - k_{MF})}{(k_{FM} + k_{MF})} \cdot \frac{1}{2} [k_r^M e^M(\lambda_{em}) - k_r^F e^F(\lambda_{em})] \right] \right\}. \quad (3)$$

Since the contribution of the second term will be small, this can be approximated to be:

$$\simeq [\epsilon^S + \epsilon^M + \epsilon^F] \cdot \tfrac{1}{2} [k_r^M e^M(\lambda_{em}) + k_r^F e^F(\lambda_{em})].$$

Thus, the spectrum of the slow component (described by $a_1[\lambda]$) is approximately the sum of the spectra from the M and F chromophores.

$$a_2(\lambda_{em}) = \epsilon^S(\lambda_{ex})\left\{k_r^S e^S(\lambda_{em}) - \frac{1}{2}[k_r^M e^M(\lambda_{em}) + k_r^F e^F(\lambda_{em})]\right.$$

$$\left. - \frac{1}{2}[k_r^M e^M(\lambda_{em}) - k_r^F e^F(\lambda_{em})]\,\frac{k_{SM} - k_{SF} + k_{MF} - k_{FM}}{k_{SM} + k_{SF} - k_{MF} - k_{FM}}\right\}. \quad (4)$$

Again, the contribution of the second term is expected to be small and we approximate this equation by

$$\simeq \epsilon^S(\lambda_{ex}) k_r \{e^S(\lambda_{em}) - \tfrac{1}{2}[e^M(\lambda_{em}) + e^F(\lambda_{em})]\}.$$

In the short-wavelength part, the spectrum described by the a_2 term will resemble the one of the S-chromophore.

The third amplitude term is given by:

$$a_3(\lambda_{em}) = \frac{k_{MF}\,\epsilon^M - k_{FM}\,\epsilon^F}{k_{MF} + k_{FM}} \cdot [k_r^M e^M(\lambda_{em}) - k_r^F e^F(\lambda_{em})]. \quad (5)$$

Thus, $a_1(\lambda_{em})$, i.e., the amplitude of the longest-lived decay component, reflects the combined spectrum of the M-chromophores and the F-chromophores and the amplitude terms $a_2(\lambda_{em})$ and $a_3(\lambda_{em})$ of the short-lived components display the difference spectra between the various chromophores. Both $a_2(\lambda_{em})$ and $a_3(\lambda_{em})$ may therefore become negative. In view of the similarity of $e^M(\lambda)$ and $e^F(\lambda)$ the function $a_3(\lambda_{em})$ is expected to be relatively small in amplitude.

Comparison with the Experimental Data

If we neglect for a while the 550-ps component of very small amplitude, the experimental fluorescence kinetics of the hexamer comes very close to the predictions of the model. Comparison of Eqs. 2–5 with the experimental time-resolved spectra results in the following assignment. The longest-lived component of 1.8 ns. is clearly the sum of the radiative and nonradiative decays (component 1 in Eq. 2, i.e., $1/\tau_1 = k_1 = k_r + k_{nr}$). Because of its short-wavelength maximum, the shortest-lived component of 10-ps lifetime is assigned to the decay of the S-chromophores (component 2 in Eq. 2, i.e., $1/\tau_2 = k_2 = k_{SF} + k_{SM}$). The middle decay component (50 ps) is assigned to the equilibration of the M and F chromophores (component 3 in Eq. 2, i.e., $1/\tau_3 = k_3 = k_{MF} + k_{FM}$) on the basis of its spectrum and lifetime.

For monomers and trimers experimentally four decay components with significant amplitudes are observed. This means that there is one component more than would be expected theoretically. This extra component probably arises from some type of heterogeneity in the sample that has been reported already (16, 30). This heterogeneity is discussed below in detail. Despite these complications the two fastest components in the trimer and the fastest component in the monomer can still be assigned as representing proper energy transfer components on the basis of both their spectra (positive and negative amplitudes are predicted by the model) and their lifetimes. At this stage we prefer to assign the 600-ps and 675-ps components in trimers and monomers, respectively, to represent the extra, inhomogeneous, component. If this assignment is correct, the components due to radiative and nonradiative decays, i.e., the ones analogous to the long-lived 1.8 ns in hexamers, would be 1.3 ns in monomers and trimers (component 1 in Eq. 2). Correspondingly, the fastest components of 47 ps (monomers) and 35 ps (trimers) would then have to be assigned to the decay of the S-chromophore(s) (component 2 in Eq. 2). The equilibration between the M and F-chromophores (component 3 in Eq. 2) is consequently assigned to the components with 200 ps (monomers) and 120 ps (trimers) lifetime.

From our kinetic analysis it follows that $k_2 = k_{SM} + k_{SF}$, represents the sum of all energy transfer rate constants from an individual S-chromophore to all M-chromophores and F-chromophores of the aggregate, while $k_3 = k_{MF} + k_{FM}$ represents the corresponding sum of all rate constants referring to transfers between M and F. According to our assignment given above, we obtain from our experimental lifetime data for k_2 and k_3 (inverse experimental lifetimes) 21 and 5 ns^{-1} in the monomer, 29 and 8 ns^{-1} in the trimer, and 100 and 20 ns^{-1} in the hexamer, respectively. Thus, with higher aggregation, both experimental rate constants for energy transfer are increasing due to the higher number of transfer processes involved and/or the availability of more favorable acceptor chromophores. Note that the corresponding value for k_2 in trimers with linker proteins has been found to be significantly higher (45 ns^{-1}) (30).

In a recent spectroscopic study of C-PC from *Mastigocladus* the β-84 chromophores have been assigned to be the F-chromophores and the β-155 the S-chromophores (17). Such an assignment appears to be consistent with our time-resolved data. However, we stress the point that at the present stage our data also do not exclude the alternative assignment of β-155 as F-chromophore. We therefore cannot presently give a final assignment. We have a slight preference also for the assignment given by reference 17. Such an assignment would, therefore, allow us to rationalize more easily the spectral changes in the long-wavelength chromophores upon association with linker peptides, which are situated in the central part on the trimers/hexamers, i.e., closest to the β-84 chromophores. (This tentative assignment is used for the presentations of Fig. 5.) A more detailed analysis based on further experimental data seems to be required to finally clarify this point. However, any final assignment would have to be consistent with the experimental findings, that the shortest-wavelength component is associated with the shortest-lived decay in all three aggregates.

Independent of the final assignment of S-chromophores and F-chromophores the doubling of k_2 upon trimer formation reflects the occurrence of two major new transfer channels depleting the S-chromophore, namely the trans-

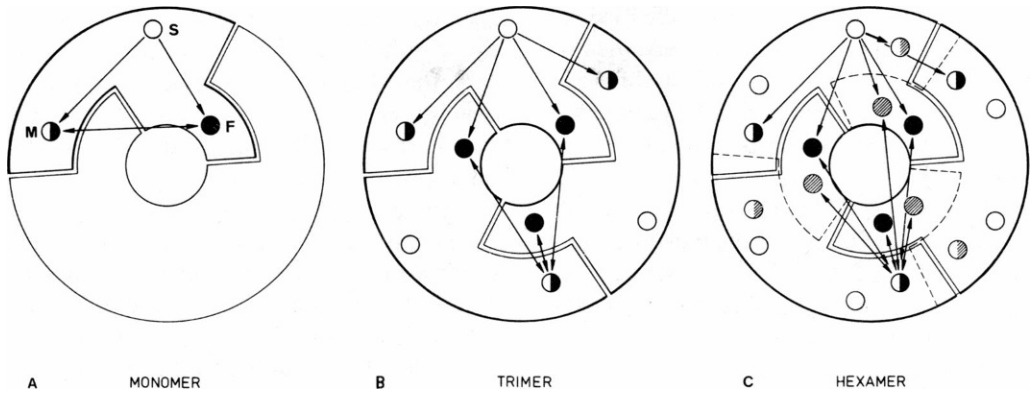

FIGURE 5 Schematic model of the energy transfer pathways in C-PC aggregates. (*A*) monomers, (*B*) trimers, and (*C*) hexamers (head-to-head configuration). Only the most relevant transfer steps are indicated by arrows. The hexamer and the trimer are schematized according to reference 45. Note that the structure of the hexamer and the assignments of the S- and F-chromophores are tentative only. S, β155 (*open circle*); M, α84 (*half-filled circle*); F, β84, (*solid circle*).

fers to the M-chromophores and F-chromophores of the neighboring monomers (see Fig. 5). These lie in comparable distances from the S-chromophore(s), as do the corresponding acceptor chromophores of the monomer (40, 41). Note that k_3 increases only from 5 to 8 ns^{-1} upon trimer formation. This would be a surprising finding if β-84 were indeed the F-chromophore, because the β-84 and the α-84 (M)-chromophore of two neighboring monomers are very close to each other (21.5 Å) in the trimeric unit according to the x-ray structure (41). In this case, perhaps a more drastic increase in k_3 would be expected when going from the monomer to the trimer, unless the orientation factor for Förster resonance transfer would be very unfavorable for this pair.

The drastic increase of k_2 in hexamers as compared with trimers may be understood in view of the close neighborhood of peripheral (α-84) M-chromophores and S-chromophores in this aggregate. The increase in k_3 is also easily rationalized since the number of possible transfer paths between M and F is roughly doubled when going from trimers to hexamers. It is not exactly known from the spectral data to what extent the transfer between M and F is asymmetric. However, it follows from Eq. 2 that there has to be a substantial asymmetry (difference in spectra) between the M and F chromophores to observe the component a_3 with the amplitude ratios found in our time-resolved spectra.

Numerical Calculations

We have calculated the predicted time-resolved component spectra of the monomers and hexamers on the basis of our kinetic model (matrix formalism), using the model spectra shown in Fig. 4. A comparison of the predicted spectra (Fig. 6) with the measured ones (Figs. 3, *A* and *C*) reveals a fairly good agreement. The calculated spectra qualitatively show all these features which are observed in the experimental data. Considering all the uncertainties in the

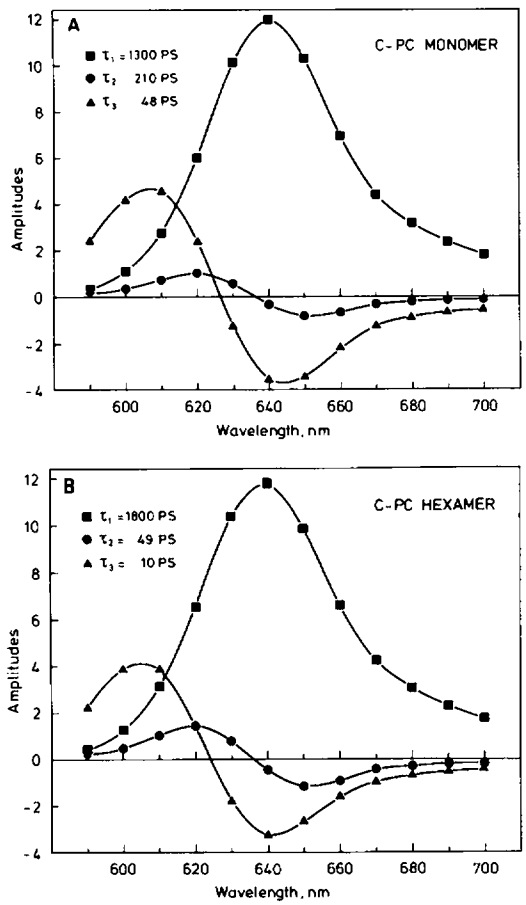

FIGURE 6 Calculated time-resolved fluorescence spectra for the monomer and the hexamer of C-PC using the following parameters (see text): *Monomer*: $k_{SM} = 2\ ns^{-1}$, $k_{SF} = 18\ ns^{-1}$; $k_{MF} = 3\ ns^{-1}$; $k_{FM} = 1\ ns^{-1}$. *Hexamer*: $k_r^{S,F} + k_{nr}^{S,F} = 0.56\ ns^{-1}$; $k_{SM} = k_{SF} = 50\ ns^{-1}$; $k_{MF} = 15\ ns^{-1}$; $k_{FM} = 5\ ns^{-1}$, $\lambda_{exc} = 590$ nm. The model spectra used for the calculation are shown in Fig. 4.

measurement as well as those in the assumed model spectra of the individual chromophores, we take this agreement as a confirmation of the validity of our model. It should be kept in mind that the model spectra of Fig. 4 are based on the data from α-subunits and β-subunits. They, therefore, will be most appropriate for the case of the monomers (17). The spectrum of the hexamers is shifted bathochromically and narrowed as compared with that of the monomers (see above). The fact that this shift and change in shape is not accounted for by the model spectra will affect, in particular, the calculated time-resolved spectrum of the fast component. For this same reason, the experimental time-resolved spectra of the hexamer as a whole are somewhat red-shifted as compared with the calculated ones.

One should note that k_2 and k_3 are the essential parameters on the energy transfer kinetics which can be obtained from the isotropic fluorescence kinetics. No information can be obtained on the rate constants of individual transfer steps between specific chromophores. Furthermore, no kinetic parameters concerning transfers between symmetrically equivalent chromophores, i.e., within the group of S, M, and F chromophores, can be deduced from isotropic fluorescence kinetics. This is reflected by the fact that these rate constants do not appear in our model (see Eqs. 2–5). Information on transfer steps between symmetrically equivalent chromophores could, in principle, be deduced from time-resolved and component-resolved anisotropy spectra. It is feasible to obtain such spectra. However, their interpretation would be extremely difficult taking into account the present uncertainties in the structural and spectral information.

Inhomogeneity in Terminal Chromophore(s)

Our kinetic analysis shows that we expect exactly three exponentials in the fluorescence kinetics of each of the different C-PC aggregates. This analysis assumes a completely homogeneous sample. In this case there would be only one long-lived component present which is determined by the radiative and nonradiative rate constants (cf. Eq. 2). At least for the monomers and the trimers we find two significant long-lived components, however. Such behavior has been described already in references 10, 16, and 29 for monomers of C-PC, and in reference 30 for trimers. Switalski and Sauer (16) attributed the occurrence of two long-lived components to the presence of a heterogeneity in the conformation of the chromophores themselves or from a heterogeneity in some of the chromophores. Our data are consistent with that interpretation. The heterogeneity could arise either from a heterogeneity in the protein moieties, which could in turn influence the chromophore(s) by a modified chromophore/protein interaction. The chromophore/protein interaction is of fundamental importance for the photophysical properties of the chromophores in phycobiliproteins (29, 42, 43, 44). We can conclude from our analysis that either the M- or the F-chromophores or both may be affected by such a heterogeneity. (Note that the long-lived component contains the contributions from both the M and F chromophores, cf. Eq. 3). This heterogeneity seems to be characteristic for the lower aggregation states of C-PC (10, 16, 29, 30). In the hexamers it is almost absent.

The lengthening of the decay time of the terminal chromophores in the hexamers also indicates a higher rigidity and/or conformational stability of the chromophores. In the hexamers this could be brought about by the interaction of the linker peptide(s) with the apoproteins and/or by the interaction of the protein moieties of the two constituent trimers. It is interesting that the long-lived fluorescence decay in the hexamers (1.8 ns) is identical within the error limits to that found in the C-PC emission region of PBS. In the PBS this component has been attributed to C-PC emission from a small amount of dissociated PBS rods (24, 26, 44). The identity of these lifetimes indicates also that hexameric units of C-PC are the functional units forming the rods in PBS of S 6301. This view is further corroborated by the fact that the fast lifetime (10 ps) found in the hexamers has been found previously also in intact PBS (23, 24, 26). This finding confirms our previous assignment of the fast ($\approx$ 10 ps) component found in PBS to s→f energy transfer.

APPENDIX A

(For a more extensive presentation, see Holzwarth A. R. and G. Suter, manuscript submitted for publication). The kinetic problem is described by a series of first order differential equations. These equations are solved using appropriate boundary conditions, i.e., initial excitations described by weighting factors that are determined by the spectral shape of the absorption and emission of the individual pigments.

Let $\bar{X}$ be the concentration vector of the different chromophores which are numbered 1 to N. K is the matrix of all rate constants for energy transfer and decay to the ground state. The system of differential equation describing the kinetics of the excited states is then

$$\partial \bar{X} / \partial t = K \cdot \bar{X}.$$

In the case of the trimers K is given by a 9 × 9 matrix. The structure of the kinetic matrix is visualized in Scheme I.

	S	S	S	M	M	M	F	F	F
S	*	*	*	*	*	*	*	*	*
S	*	*	*	*	*	*	*	*	*
S	*	*	*	*	*	*	*	*	*
M	*	*	*	*	*	*	*	*	*
M	*	*	*	*	*	*	*	*	*
M	*	*	*	*	*	*	*	*	*
F	*	*	*	*	*	*	*	*	*
F	*	*	*	*	*	*	*	*	*
F	*	*	*	*	*	*	*	*	*

Scheme I

Due to the threefold rotation axis (C_3 symmetry) the structure of the 3 × 3 subblocks is very simple. Two cases have to be considered, i.e., diagonal and off-diagonal subblocks.

The elements of the diagonal subblocks are

$$\begin{matrix} s & k & k \\ k & s & k \\ k & k & s \end{matrix}$$

where k is the rate constant for transfers between the symmetrically equivalent chromophores and s is the negative sum of all processes depleting the corresponding chromophore including energy transfer and decay to the ground state. (Note that according to this definition, $s + 2k$ is independent of k [see below].)

The off-diagonal subblocks also reflect the threefold symmetry of the trimer:

$$\begin{matrix} k^0 & k^- & k^+ \\ k^+ & k^0 & k^- \\ k^- & k^+ & k^0 \end{matrix}$$

The superscripts ^{0}, $^-$, and $^+$ denote transfers to the three symmetrically equivalent accepting chromophores. Note that k, s, k^0, k^-, k^+ values in different 3 × 3 subblocks are different.

Making use of the assumed symmetry of the aggregate, the kinetic matrix may be split into several noninteracting blocks, i.e., blocks with no nonzero off-diagonal elements in common. This is done using a symmetry adapted concentration vector, $\overline{X}$, which is related to $\overline{X}$ by

$$\overline{X}' = C\,\overline{X}.$$

K then transforms according to

$$K' = C\,K\,C^{-1}.$$

The transformation matrix C may be obtained directly from the character table of the rotation group formed by the symmetrically equivalent chromophores.

As an example, the transformation taking into account only the threefold symmetry axis of the trimers is carried out below. In this case the elements of the transformation matrix C are zero except for those in the 3 × 3 subblocks along the diagonal which are given by the character table of the symmetry group C_3

$$\begin{matrix} 1 & 1 & 1 \\ 2 & -1 & -1 \\ 0 & 1 & -1 \end{matrix}$$

(Note that positive and negative linear combinations have been formed within the two-dimensional E-representation of the symmetry group C_3; this representation is more appropriate for our purposes.)

After transformation the diagonal subblocks in K' become

$$\begin{matrix} s + 2k & 0 & 0 \\ 0 & s - k & 0 \\ 0 & 0 & s - k \end{matrix}$$

and the off-diagonal subblocks

$$\begin{matrix} k^0 + k^- + k^+ & 0 & 0 \\ 0 & k^0 - (k^-/2) - (k^+/2) & \cdot\ (3k^-/2) - (3k^+/2) \\ 0 & (k^+/2) - (k^-/2) & k^0 - (k^-/2) - (k^+/2). \end{matrix}$$

Only the first rows and columns of these subblocks belong to the totally symmetric part of K'; the others vanish for an isotropic fluorescence experiment. This can be visualized most easily by looking at the symmetry adapted concentration vector. After carrying out the transformation, for example, the three symmetrically equivalent S-chromophores (S-species) denoted S_1, S_2, and S_3, will turn into the three new pseudo-species ($S_1 + S_2 + S_3$), ($2S_1 - S_2 - S_3$), and ($S_2 - S_3$), respectively. Since the three equivalent S-species cannot be distinguished in an isotropic fluorescence experiment and since all of them have the same concentration and the same detection possibility, only the first pseudo-species, i.e., ($S_1 + S_2 + S_3$), can be observed in the fluorescence decay. The others are zero at all times. This would, of course, not be valid when the anisotropy decay is being measured. In this case the pseudo-species 2 and 3 can be observed. Analogous arguments hold for the groups of M and F chromophores.

For the reasons given above the dimension of the relevant kinetic matrix K'_{ts} is only three. The matrix equation is then solved for the eigenvalues (rate constants) and the eigenvectors (amplitudes). For the hexamers the procedure to reduce the 18 × 18 matrix to a 3 × 3 matrix is analogous. The transformation matrix in this case is obtained from the character table of the symmetry group D_3. Thus, all aggregation states are described by the same formal kinetic equations.

We thank Mrs. A. Keil, Mr. U. Pieper, Mr. K. Kerpen, and Mr. H.-V. Seeling for able technical assistance. We are indebted to Dr. Hensel, Botanisches Institut der Universität München, for carrying out the analytical ultracentrifugation measurements. We also thank Prof. K. Schaffner for his interest and continuing support of this work and Prof. K. Sauer for critically reading the manuscript.

Received for publication 12 May 1986 and in final form 25 July 1986.

REFERENCES

1. Holzwarth, A. R., J. Wendler, and W. Wehrmeyer. 1983. Studies on chromophore coupling in isolated phycobiliproteins. I. Picosecond fluorescence kinetics of energy transfer in phycocyanin 645 from *Chroomonas sp. Biochim. Biophys. Acta.* 724:388–395.
2. Gantt, E. 1980. Structure and function of phycobilisomes: light harvesting pigment complexes in red and blue-green algae. *Int. Rev. Cytol.* 66:45–80.
3. Gantt, E. 1981. Phycobilisomes. *Ann. Rev. Plant Physiol.* 32:327–347.
4. Scheer, H. 1982. Phycobiloproteins: molecular aspects of a photosynthetic antenna system. *In* Light Reaction Path of Photosynthesis. Fong, F. K., editor. Springer-Verlag, Berlin. 7–45.
5. Glazer, A. N. 1983. Comparative biochemistry of photosynthetic light-harvesting systems. *Ann. Rev. Biochem.* 52:125–157.
6. Wehrmeyer, W. 1983. Organization and composition of cyanobacterial and rhodophycean phycobilisomes. G. C. Papageorgiou and L. Packer, editors. *In* Photosynthetic Prokaryotes. Elsevier Science Publishing Co. Inc., Amsterdam, New York. 1–22.
7. Glazer, A. N., S. Fang, and D. M. Brown. 1973. Spectroscopic properties of C-phycocyanin and its alpha and beta subunits. *J. Biol. Chem.* 248:5679–5685.
8. MacColl, R., and D. S. Berns. 1981. Biliproteins: some relationships among aggregation states, spectra, and excitation-energy transfer. *Isr. J. Chem.* 21:296–300.

9. Lee, J. J., and D. S. Berns. 1968. Protein aggregation. Studies of larger aggregates of C-phycocyanin. *Biochem. J.* 110:457–464.
10. Hefferle, P., P. Geiselhart, T. Mindl, S. Schneider, W. John, and H. Scheer. 1984. Time-resolved polarized fluorescence of C-phycocyanin and its subunits from *Mastigocladus laminosus*. *Z. Naturforsch.* 39c:606–616.
11. Yu, M. -H., and A. N. Glazer. 1982. Cyanobacterial phycobilisomes. Role of the linker polypeptides in the assembly of phycocyanin. *J. Biol. Chem.* 257:3429–3433.
12. Glazer, A. N., D. J. Lundell, G. Yamanaka, and R. C. Williams. 1983. The structure of a simple phycobilisome. *Ann. Microbiol.* 134B:159–180.
13. Lundell, D. J., R. C. Williams, and A. N. Glazer. 1981. Molecular architecture of a light harvesting antenna. In vitro assembly of the rod substructures of *Synechococcus 6301* phycobilisomes. *J. Biol. Chem.* 256:3580–3592.
14. Dale, R. E., and F. W. J. Teale. 1970. Number and distribution of chromophore types in native phycobiliproteins. *Photochem. Photobiol.* 12:99–117.
15. Grabowski, J., and E. Gantt. 1978. Photophysical properties of phycobiliproteins from phycobilisomes: fluorescence lifetimes, quantum yield, and polarization spectra. *Photochem. Photobiol.* 28:39–45.
16. Switalski, S. C., and K. Sauer. 1984. Energy transfer among the chromophores of C-phycocyanin from *Anabaena variabilis* using steady state and time-resolved fluorescence spectroscopy. *Photochem. Photobiol.* 40:423–427.
17. Mimuro, M., P. Füglistaller, R. Rümbeli, and H. Zuber. 1986. Functional assignment of chromophores and energy transfer in C-phycocyanin isolated from the thermophilic cyanobacterium *Mastigocladus laminosus*. *Biochim. Biophys. Acta.* 848:155–166.
18. Scheer, H. 1985. Excitation transfer in phycobiliproteins. *In* Encyclopedia of Plant Physiology: Photosynthesis III. L. A. Staehelin and C. J. Arntzen, editors. Springer-Verlag, Berlin, Heidelberg. 327–337.
19. Karukstis, K. K., and K. Sauer. 1983. Fluorescence decay kinetics of chlorophyll in photosynthetic membranes. *J. Cell. Biochem.* 23:131–158.
20. Kobayashi, T., E. O. Degenkolb, R. Bersohn, P. M. Rentzepis, R. MacColl, and D. S. Berns. 1979. Energy transfer among the chromophores in phycocyanins measured by picosecond kinetics. *Biochemistry* 18:5073–5078.
21. Doukas, A. G., F. Pellegrino, D. Wong, V. Stefanic, J. Buchert, R. R. Alfano, and B. A. Zilinskas. 1981. Picosecond absorption and fluorescence studies of the isolated phycobiliproteins from the blue-green alga *Nostoc sp.* *In* Photosynthesis I. Photophysical Processes—Membrane Energization. G. Akoyunoglou, editor. Balaban International Science Services, Philadelphia, 59–68.
22. Doukas, A. G., V. Stefancic, J. Buchert, R. R. Alfano, and B. A. Zilinskas, 1981. Exciton annihilation in the isolated phycobiliproteins from the blue-green alga *Nostoc sp.* using picosecond absorption spectroscopy. *Photochem. Photobiol.* 34:505–510.
23. Gillbro, T., A. Sandström, V. Sundström, and A. R. Holzwarth. 1983. Polarized absorption picosecond kinetics as a probe of energy transfer in phycobilisomes of *Synechococcus 6301*. *FEBS (Fed. Eur. Biochem. Soc.)* 162:64–68.
24. Gillbro, T., A. Sandström, V. Sundström, J. Wendler, and A. R. Holzwarth, 1985. Picosecond study of energy transfer kinetics in phycobilisomes of *Synechococcus 6301* and the mutant *AN 112*. *Biochim. Biophys. Acta.* 808:52–65.
25. Hefferle, P., M. Nies, W. Wehrmeyer, and S. Schneider. 1983. Picosecond time-resolved fluorescence study of the antenna system isolated from *Mastigocladus laminosus* Cohn. II. Constituent biliproteins in various forms of aggregation. *Photobiochem. Photobiophys.* 5:325–334.
26. Suter, G. W., P. Mazzola, J. Wendler, and A. R. Holzwarth. 1984. Fluorescence decay kinetics in phycobilisomes from the blue-green alga *Synechococcus 6301*. *Biochim. Biophys. Acta.* 766:269–276.
27. Wehrmeyer, W., J. Wendler, and A. R. Holzwarth. 1985. Biochemical and functional characterization of a peripheral unit of the phycobilisomes from *Porphyridium cruentum*. Measurement of picosecond energy transfer kinetics. *Eur. J. Cell Biol.* 36:17–23.
28. Wong, D., F. Pellegrino, R. R. Alfano, and B. A. Zilinskas. 1981. Fluorescence relaxation kinetics and quantum yield from the isolated phycobiliproteins of the blue-green alga *Nostoc sp.* measured as a function of single picosecond pulse intensity. *Photochem. Photobiol.* 33:651–662.
29. Hefferle, P., W. John, H. Scheer, and S. Schneider. 1984. Thermal denaturation of monomeric and trimeric phycocyanins studied by static and polarized time-resolved fluorescence spectroscopy. *Photochem. Photobiol.* 39:221–232.
30. Wendler, J., W. John, H. Scheer, and A. R. Holzwarth. 1986. Energy transfer kinetics in trimeric C-Phycocyanin studied by picosecond fluorescence kinetics. *Photochem. Photobiol.* 44:79–85.
31. Hanzlik, C. A., L. E. Hancock, R. S. Knox, D. Guard-Friar, and R. MacColl. 1985. Picosecond fluorescence spectroscopy of the biliprotein phycocyanin 612. Direct evidence for fast energy transfer. *J. Lumin.* 34:99–106.
32. Knorr, F. J., and J. M. Harris. 1981. Resolution of multicomponent fluorescence spectra by an emission wavelength—decay time data matrix. *Anal. Chem.* 53:272–276.
33. Knutson, J. R., J. M. Beechem, and L. Brand. 1983. Simultaneous analysis of multiple fluorescence decay curves: a global approach. *Chem. Phys. Lett.* 102:501–507.
34. Neufeld, G. J., and A. F. Riggs. 1969. Aggregation properties of C-phycocyanin from *Anacystis nidulans*. *Biochim. Biophys. Acta.* 181:234–243.
35. MacColl, R., J. J. Lee, and D. S. Berns. 1971. Protein Aggregation in C-Phycocyanin Studies at very low concentrations with the photoelectric scanner of the ultracentrifuge. *Biochem. J.* 122:421–426.
36. Laemmli, U. K. 1970. Cleavage of structural proteins during the assembly of the head of bacteriophage T4. *Nature (Lond.)* 227:680–685.
37. Glazer, A. N. 1982. Phycobilisomes: structure and dynamics. *Ann. Rev. Microbiol.* 36:173–198.
38. Holzwarth, A. R., H. Lehner, S. E. Braslavsky, and K. Schaffner. 1978. Phytochrome models II: The fluorescence of biliverdin dimethyl ester. *Liebigs Ann. Chem.* 2002–2017.
39. Marquardt, D. W. 1963. An algorithm for least-squares estimation of nonlinear parameters. *J. Soc. Ind. Appl. Math.* 11:431–441.
40. Schirmer, T. 1985. Roentgenstrukturanalyse des lichtsammelnden. Phycobiliproteins C-Phycocyanin von *Mastigocladus laminosus*. Ph.D. Thesis, TU München. 1–92.
41. Schirmer, T., W. Bode, R. Huber, W. Sidler, and H. Zuber. 1985. X-ray crystallographic structure of the light-harvesting biliprotein C-phycocyanin from the thermophilic cyanobacterium *Mastigocladus laminosus* and its resembleance to globin structures. *J. Mol. Biol.* 184:257–277.
42. Braslavsky, S. E., A. R. Holzwarth, and K. Schaffner. 1983. Conformation analysis, photophysics and photochemistry of bile pigments. Bilirubin and biliverdin dimethyl esters and related linear tetrapyrroles. *Angew. Chemie* 95:670–689.
43. Lehner, H., and H. Scheer. 1983. Circular-dichroism of C-phycocyanin: origin of optical activity in denatured biliproteins and evidence for an intermediate during unfolding. *Z. Naturforsch.* C 38:353–358.
44. Holzwarth, A. R. 1985. Energy transfer kinetics in phycobilisomes. *In* Antennas and Reaction Centers of Photosynthetic Bacteria. M. E. Michel-Beyerle, editor. Springer-Verlag, Berlin. 45–52.
45. Schirmer, T., W. Bode, R. Huber, W. Sidler, and H. Zuber. 1985. The crystal and molecular structure of C-Phycocyanin from *Mastigocladus laminosus* and its implications for function and evolution. *In* Optical Properties and Structure of Tetrapyrroles. G. Blauer and H. Sund, editors. Walter de Gruyter, Berlin, New York. 446–449.